Chinese Journal of Natural Medicines

Benzyl sulfide, sulfoxide and sulfinate metabolites from *Gastrodia elata* and their synthesis, derivatization and anti-inflammatory activity

Chengbo Xu, Lei Wang, Xue Zhou, Shuai Shao, Chengjuan Chen, Xiaoqiang Lei, Tiantai Zhang, Jiachen Zi, Jiangong Shi, Qinglan Guo

Citation: Chengbo Xu, Lei Wang, Xue Zhou, Shuai Shao, Chengjuan Chen, Xiaoqiang Lei, Tiantai Zhang, Jiachen Zi, Jiangong Shi, Qinglan Guo, Benzyl sulfide, sulfoxide and sulfinate metabolites from *Gastrodia elata* and their synthesis, derivatization and anti-inflammatory activity, Chinese Journal of Natural Medicines, 2026, 24(3), 365-372. doi: 10.1016/S1875-5364(26)61110-7.

View online: https://doi.org/10.1016/S1875-5364(26)61110-7

Chinese Journal of Natural Medicines 24 (2026) 365-372

Contents lists available at ScienceDirect

Chinese Journal of Natural Medicines

journal homepage: www.cjnmcpu.com/

Original article

Benzyl sulfide, sulfoxide and sulfinate metabolites from *Gastrodia elata* and their synthesis, derivatization and anti-inflammatory activity

Chengbo Xu[Δ], Lei Wang[Δ], Xue Zhou, Shuai Shao, Chengjuan Chen, Xiaoqiang Lei, Tiantai Zhang, Jiachen Zi[*], Jiangong Shi[*], Qinglan Guo[*]

State Key Laboratory of Bioactive Substance and Function of Natural Medicines, Institute of Materia Medica, Chinese Academy of Medical Sciences and Peking Union Medical College, Beijing 100050, China

ARTICLE INFO

Article history:
Received 9 January 2025
Revised 1 April 2025
Accepted 3 June 2025
Available online 20 February 2026

Keywords:
Gastrodia elata
Sulfur-bearing benzyl metabolites
Synthesis
Anti-inflammatory activity

ABSTRACT

Five novel sulfur-containing benzyl metabolites, designated as gastrabenzylsulfoxides A and B (**1** and **2**), gastrabenzylsulfinate A (**3**) and gastrabenzylsulfides A and B (**4** and **5**), along with four known compounds (**6**–**9**), were isolated from the aqueous extracts of *Gastrodia elata*. Compounds **1** and **4** are 4-hydroxy-3-(4′-hydroxybenzyl)benzyl-substituted sulfoxide and sulfide, respectively, which are unprecedented in natural products. Compound **3** represents a rare sulfinate. Several isolates and their sulfone and disulfide analogs (**10**–**13**) were synthesized to evaluate their anti-inflammatory activity. Notably, the synthesized sulfone **10** demonstrated significant alleviation of symptoms in multiple *in vivo* inflammatory models.

1. Introduction

The steamed and dried rhizomes of *Gastrodia elata* Blume (Orchidaceae), referred to as Tianma in traditional Chinese medicine, have been widely utilized for treating various nervous disorders and inflammation-related diseases, such as rheumatism and arthralgia [1, 2]. To date, over 130 compounds have been isolated from this plant. The majority of these compounds are benzyl-bearing derivatives, including simple benzyl alcohols, polybenzyls (e.g., dimers, trimers, tetramers, and pentamers), and sulfur-bearing benzyl derivatives (such as sulfides, sulfoxides, sulfones, and benzyl-substituted sulfur-bearing amino acids and oligopeptides) [1–11]. Many benzyl-bearing compounds exhibit neuroprotective activities. For instance, gastrodin, a major metabolite of *G. elata*, has been shown to alleviate lead-induced brain injury in mice by regulating the Wnt/Nrf2 pathway [12]. Additionally, **20C**, a polybenzyl tetramer, exhibits potent neuroprotection through mechanisms involving multiple pathways [13–16]. Furthermore, divanillyl sulfone has been reported to ameliorate chronic neuropathic pain by suppressing the activation of the nod-like receptor thermal protein domain associated protein 3 (NLRP3) inflammasome [17].

Although extensive research has explored the neuroprotective effects of *G. elata* metabolites, few studies have focused on their anti-inflammatory properties. Notably, many benzyl-bearing metabolites from *G. elata* act as neuroprotection agents *via* inflammatory mechanisms. For example, gastrodin can activate NLRP3 inflammasome [18], while 3,4-dihydroxybenzaldehyde modulates the expression of anti-inflammatory cytokines and inhibits the MAPK and NF-*κ*B pathways [19]. These findings suggest that benzyl-bearing metabolites also play crucial roles in the anti-inflammatory effects of *G. elata*. Given that numerous sulfur-containing natural products possess significant anti-inflammatory activities [20], we investigated sulfur-containing benzyl derivatives from the aqueous extracts of *G. elata*, leading to the isolation of five new and four known compounds of this class (Fig. 1). Among them, **1**–**3** are racemates that were separated using chiral chromatography. Compounds **1** and **4** are 4-hydroxy-3-(4′-hydroxybenzyl)benzyl-substituted sulfoxide and sulfide, respectively, marking the first discovery of natural compounds with sulfur-bearing polybenzyl moieties. Compound **3** is a rare sulfinate. The isolates and their analogs (**10**–**13**) (Fig. 1) were synthesized for *in vivo* evaluation of their anti-inflammatory activities, and **10** showed the highest activity.

2. Results and discussion

2.1. Structural elucidation of the isolates

Compound **1**, obtained as yellowish gum with $[\alpha]_D^{20} \approx 0$ (*c* 0.46, MeOH), exhibited a molecular formula of $C_{21}H_{20}O_4S$ according to its sodium adduct at *m/z* 391.0991 $[M + Na]^+$ (Calcd. for $C_{21}H_{20}O_4SNa$, 391.0975) in its high-resolution electrospray ionization mass spectrometry (HR-ESI-MS) spectrum. The ^1H nuclear magnetic resonance (NMR) spectrum of **1** (Table 1) showed three groups of the characteristic signals attributable to a trisub-

* Corresponding author.
E-mail addresses: zijiachen@imm.ac.cn (J. Zi); shijg@imm.ac.cn (J. Shi); guonina@imm.ac.cn (Q. Guo)
Δ These authors contributed equally to this work.

https://doi.org/10.1016/S1875-5364(26)61110-7

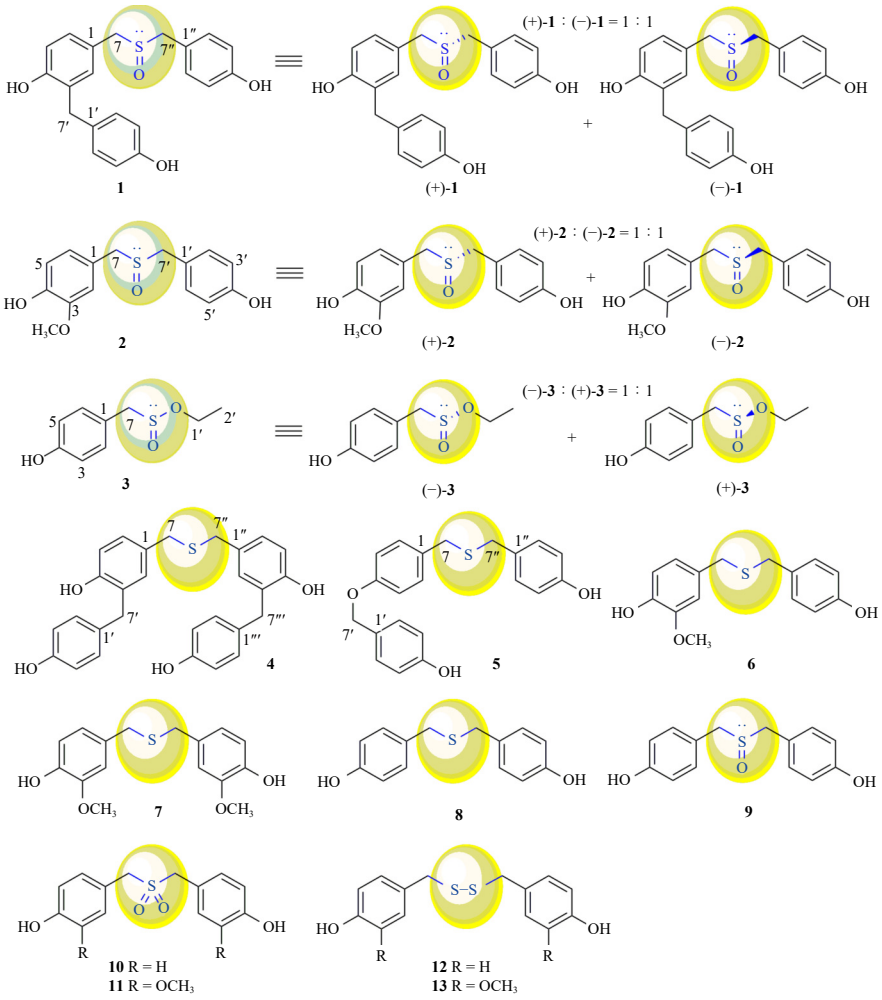

Fig. 1 Chemical structures of compounds **1**–**13**.

stituted phenyl [δ_H 7.02 (br s, 1H), 7.01 (br d, J = 8.4 Hz, 1H) and 6.83 (d, J = 8.4 Hz, 1H)] and two disubstituted phenyls [δ_H 7.08 (d, J = 8.4 Hz, 2H) and 6.71 (d, J = 8.4 Hz, 2H); δ_H 7.13 (d, J = 8.4 Hz, 2H) and 6.81 (d, J = 8.4 Hz, 2H)]. The heteronuclear single quantum coherence (HSQC) experiment assigned one-bond linkages between hydrogens and carbons, indicating the presence of three methylene groups [δ_H 3.91 (d, J = 12.6 Hz, 1H) and 3.71 (d, J = 12.6 Hz, 1H), δ_C 57.4; δ_H 3.86 (s, 2H), δ_C 35.3; δ_H 3.92 (d, J = 12.6 Hz, 1H) and 3.73 (d, J = 12.6 Hz, 1H), δ_C 57.2]. Heteronuclear multiple bond correlations (HMBCs) from H_2-7 to C-1 and C-2/C-6, from H_2-7′ to C-1′, C-2′/C-6′, C-4 and C-3/C-5, from O*H*-4 to C-3/5 and C-4, and from O*H*-4′ to C-3′/5′ and C-4′, constructed a moiety of 3-(4′-hydroxybenzyl)-4-hydroxybenzyl. Additional HMBCs from H_2-7″ to C-1″ and C-2″/C-6″ and from O*H*-4″ to C-3″/5″ and C-4″ indicated the presence of a 4-hydroxybenzyl group (Fig. 2). Subsequently, 3-(4′-hydroxybenzyl)-4-hydroxybenzyl and 4-hydroxybenzyl were linked *via* a sulfoxide group, supported by the HMBCs from H_2-7 to C-7″ and H_2-7″ to C-7 (Fig. 2), consistent with the molecular formula of **1**. Thus, the structure of **1** was determined, and named gastrabenzylsulfoxide A. Using a semi-preparative chiral column, **1** was separated into (+)-**1** and (−)-**1** in a 1∶1 ratio (Fig. 3). The experimental CD spectra of (+)-**1** and (−)-**1** matched the theoretically calculated ECD spectra of the *S* and *R* enantiomers (Fig. 4), respectively.

Compound **2** was isolated as a white amorphous powder. Similar to **1**, **2** may also be a racemate, as evidenced by its $[\alpha]_D^{20}$ ≈ 0 (*c* 0.87, MeOH). The molecular formula of **2** was determined as $C_{15}H_{16}O_4S$ based on HR-ESI-MS and NMR data (Table 1). The ^{1}H NMR spectrum (Table 1) showed two sets of signals assignable to a trisubstituted phenyl [δ_H 6.95 (br s, 1H), 6.81 (overlapped, 1H) and 6.81 (overlapped, 1H)] and a disubstituted phenyl [δ_H 7.18 (d, J = 8.4 Hz, 2H) and 6.83 (d, J = 8.4 Hz, 2H)]. Furthermore, the HMBC correlations from H_2-7 to C-1 and C-2/C-6, from H_2-7′ to C-1′ and C-2′/C-6′, from O*H*-4 to C-3/5 and C-4, from O*H*-4′ to C-3′/5′ and C-4′, and from H_3-OCH_3 to C-3′ (Fig. 2), suggested that these two phenyl groups cprrespond to a 4-hydroxy-3-methoxybenzyl and a 4-hydroxybenzyl. We inferred that these two moieties were linked *via* a sulfoxide group based on HMBCs H_2-7 to C-7″ and H_2-7″ to C-7 (Fig. 2), together with the molecular formula of **2**. Thus, the structure of **2** was elucidated and named gastrabenzylsulfoxide B. After its two enantiomers were separated, the configurations of (+)-**2** and (−)-**2** with a 1∶1 ratio (Fig. 3) were determined to be *S* and *R*, respectively, by comparing their experimental and calculated ECD spectra (Fig. 4).

Compound **3** was obtained as yellowish gum with $[\alpha]_D^{20}$ ≈ 0 (*c* 0.79, MeOH). Its molecular formula, $C_9H_{12}O_3S$, was determined by HR-ESI-MS (*m/z* 201.0577 $[M + H]^+$). The ^{1}H and ^{13}C NMR data (Table 1) indicated the presence of a 4-hydroxybenzyl [δ_H 7.20 (d, J = 8.4 Hz, 2H), 6.83 (d, J = 8.4 Hz, 2H), 3.98 (d, J = 13.2 Hz, 1H) and 3.85 (d, J = 13.2 Hz, 1H); δ_C 121.3, 132.6, 116.2, 158.2 and 63.9] and an ethyl [δ_H 1.23 (t, J = 7.2 Hz, 3H), 3.98 (dq, J = 10.8 and 7.2 Hz, 1H) and 4.04 (dq, J = 10.8 and 7.2 Hz, 1H); δ_C 16.1 and 64.4]. We inferred that the structure of **3** is ethyl 4-hydroxybenzylsulfinate based on its molecular formula and the chemical shifts of C-7 and C-1′. The inequivalence of two pairs of geminal protons on C-7 and C-1′ further supports the linkage of these carbons to the chiral sulfinate. Subsequently, **3** was synthesized to validate its structure (Scheme 1). Thus, the structure

Table 1 NMR spectroscopic data for compounds **1**–**5**[a].

No.	**1**		**2**		**3**		**4**		**5**	
	δ_C, type	δ_H (*J* in Hz)	δ_C, type	δ_H (*J* in Hz)	δ_C, type	δ_H (*J* in Hz)	δ_C, type	δ_H (*J* in Hz)	δ_C, type	δ_H (*J* in Hz)
1	123.0, C		123.6, C		121.3, C		130.1, C		131.4, C	
2	133.1, CH	7.02 br s	114.4, CH	6.95 br s	132.6, CH	7.20 d (8.4)	131.8, CH	6.95 d (1.8)	130.8, CH	7.22 d (8.4)
3	129.6, C		148.3, C		116.2, CH	6.83 d (8.4)	129.1, C		115.5, CH	6.94 d (8.4)
4	155.6, C		147.4, C		158.2, C		154.6, C		158.9, C	
5	116.0, CH	6.83 d (8.4)	115.8, CH	6.81 overlapped	116.2, CH	6.83 d (8.4)	115.8, CH	6.78 d (7.8)	115.5, CH	6.94 d (8.4)
6	129.9, CH	7.01 br d (8.4)	123.9, CH	6.81 overlapped	132.6, CH	7.20 d (8.4)	128.5, CH	6.91 dd (7.8, 1.8)	130.8, CH	7.22 d (8.4)
7a	57.4, CH_2	3.91 d (12.6)	58.0, CH_2	3.98 d (12.6)	63.9, CH_2	3.98 d (13.2)	35.5, CH_2	3.45 s	35.5, CH_2	3.56 s
7b		3.71 d (12.6)		3.78 d (12.6)		3.85 d (13.2)		3.45 s		3.56 s
1′	132.6, C		123.2, C		64.4, CH_2	4.04 dq (10.8, 7.2)	132.8		129.1, C	
						3.98 dq (10.8, 7.2)				
2′	130.6, CH	7.08 d (8.4)	132.3, CH	7.18 d (8.4)	16.1, CH_3	1.23 t (7.2)	130.6	7.08 d (8.4)	130.3, CH	7.31 d (8.4)
3′	115.9, CH	6.71 d (8.4)	116.2, CH	6.83 d (8.4)			115.8	6.73 d (8.4)	115.9, CH	6.85 d (8.4)
4′	156.4, C		158.1, C				156.3		158.0, C	
5′	115.9, CH	6.71 d (8.4)	116.2, CH	6.83 d (8.4)			115.8	6.73 d (8.4)	115.9, CH	6.85 d (8.4)
6′	130.6, CH	7.08 d (8.4)	132.3, CH	7.18 d (8.4)			130.6	7.08 d (8.4)	130.3, CH	7.31 d (8.4)
7′a	35.3, CH_2	3.86 s	57.6, CH_2	3.98 d (12.6)			35.3	3.84 s	70.4, CH_2	4.98 s
7′b				3.78 d (12.6)				3.84 s		
1″	123.0, C								130.0, C	7.13 d (8.4)
2″	132.3, CH	7.13 d (8.4)							130.9, CH	6.78 d (8.4)
3″	116.2, CH	6.81 d (8.4)							115.9, CH	
4″	158.1, C								157.1, C	6.78 d (8.4)
5″	116.2, CH	6.81 d (8.4)							115.9, CH	7.13 d (8.4)
6″	132.3, CH	7.13 d (8.4)							130.9, CH	3.59 s
7″a	57.2, CH_2	3.92 d (12.6)							35.7, CH_2	3.59 s
7″b		3.73 d (12.6)								
OCH_3			56.2, CH_3	3.83 s						
OH-4		8.45 br s		7.66 br s		8.45 br s		8.18 br s		
OH-4′		8.10 br s		8.43 br s				8.18 br s		8.28 br s
OH-4″		8.47 br s								8.39 br s

[a] NMR data (δ) were measured in acetone-d_6 at 600 MHz for **1**–**5**. Coupling constants (*J*) in Hz are given in parentheses. The assignments were based on DEPT, ^{1}H–^{1}H COSY, HSQC, and HMBC experiments, and the data were presented as calculated using the solvent peak as the reference.

of **3** was confirmed and named gastrabenzylsulfinate A. **3** was also separated into a pair of enantiomers, (−)-**3** and (+)-**3**, in approximately a 1∶1 ratio (Fig. 3). Their configurations were determined to be *S* and *R*, respectively, by comparing their measured and calculated ECD spectra (Fig. 4). Sulfur-containing natural products isolated to date primarily include sulfides, disulfides, trisulfides, sulfoxides, sulfones, sulfonates, sulfates, sulfonamides, sulfamates, thioesters, thioamides, isothiocyanates, thiazoles and thiazolines [21], with few sulfinates reported.

Compound **4**, a white amorphous powder, has a molecular formula of $C_{28}H_{26}O_4S$, as determined by HR-ESI-MS and NMR data (Table 1). The NMR data (Table 1) are similar to those of 3-(4′-hydroxybenzyl)-4-hydroxybenzyl in **1**, with the main differences being the chemical shifts of C-1 and C-7 [δ_C 130.1 (C-1) and 35.5 (C-7) for **4**; δ_C 123.0 (C-1) and 57.4 (C-7) for **1**]. This observation suggested that **4** contains 3-(4′-hydroxybenzyl)-4-hydroxybenzyl group(s), which was confirmed by HMBC experiments (Fig. 2). However, the oxidation states of sulfur atoms differ between **1** and **4**. Based on the molecular formula of **4**, we inferred a symmetric structure, where two 3-(4′-hydroxybenzyl)-4-hydroxybenzyl moieties are linked *via* a thioether bond. This hypothesis was further supported by HMBCs between C-7/C-7" and H_2-7"/H_2-7 (Fig. 2) and their respective chemical shifts. Thus, the structure of **4** was assigned as bis-[4-hydroxy-3-(4′-hydroxybenzyl)benzyl]sulfide and named gastrabenzylsulfide A.

Compound **5** was obtained as a white amorphous powder. Its molecular formula was determined to be $C_{21}H_{20}O_3S$ based on HR-ESI-MS and NMR data (Table 1). The ^{1}H and ^{13}C NMR spectra

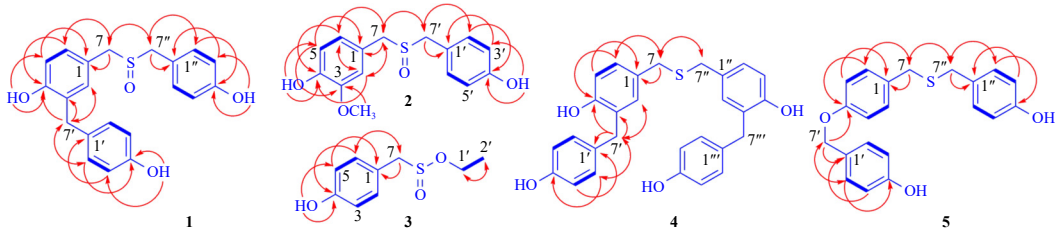

Fig. 2 Key $^{1}H-^{1}H$ COSY (thick lines) and HMBCs (red arrows) of compounds **1**–**5**.

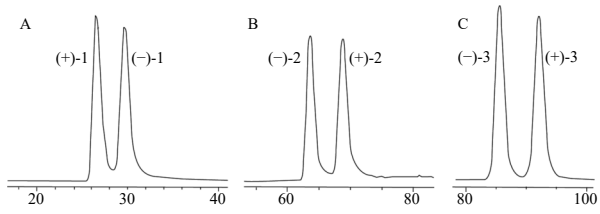

Fig. 3 The HPLC chromatograms of **1** (A), **2** (B) and **3** (C) on Chiralpak AD-H column (5 μm, 250 mm × 10 mm; *T* 23 °C). (A and B) Flow rate: 1.4 mL·min^{-1}; mobile phase: *n*-hexane–*i*PrOH mixture (3∶1, *V*/*V*); (C) Flow rate: 1.3 mL·min^{-1}; mobile phase: *n*-hexan–*i*PrOH mixture (9∶1, *V*/*V*).

(Table 1) revealed three sets of signals, each attributable to three *p*-oxybenzyls. These assignments were confirmed by HMBCs from O*H*-4′ to C-3′/5′ and C-4′, from O*H*-4″ to C-3″/5″ and C-4″, from H_2-7 to C-1 and C-2/C-6, from H_2-7′ to C-1′ and C-2′/C-6′, and from H_2-7″ to C-1″ and C-2″/C-6″ (Fig. 2). Additionally, these three moieties were shown to be tethered together through HMBCs from H_2-7/H_2-7″ to C-7″/C-7 and from H_2-7′ to C-4 (Fig. 2). Therefore, the structure of **5** was determined as 4-(4′-hydroxybenzyloxy)benzyl 4-hydroxybenzyl sulfide and named gastrabenzylesulfide B.

Four known compounds (**6**–**9**) were identified as 4-hydroxybenzyl 4-hydroxy-3-methoxybenzyl sulfide [22], bis-vanillyl sulfide [23], bis-(4-hydroxybenzyl) sulfide [24], and bis-(4-hydroxybenzyl) sulfoxide [11].

2.2. Anti-inflammatory effects and cytotoxicities of *7* and the synthetic analogs in vitro

The anti-inflammatory activities of the isolates were evaluated using a cellular model. At a concentration of 10 μg·mL^{-1}, only **7** significantly inhibited LPS-induced production of IL-6 and TNF-α, with the inhibition ratios of 70.8% and 75.3%, respectively. To obtain sufficient quantities of **7** and generate structurally diverse sulfur-containing benzyl derivatives for further bioassays, we synthesized **7** and four other compounds, including two sulfones (**10** and **11**) and two disulfides (**12** and **13**). Both **10** and **11** exhibited significant inhibitory activities against LPS-induced production of IL-6 and TNF-α *in vitro* at 10 μg·mL^{-1}, with inhibition ratios of 60.8% and 74.0%, and 51.6% and 67.8% (Table S4), respectively. To ensure that **7**, **10**, and **11** warranted further evaluation in animal models, their cytotoxicities were assessed using BV2 cell lines. **10** and **11** demonstrated noncytotoxic profiles, with cell viabilities exceeding 88.5% at 20 μg·mL^{-1} (Table S5). In contrast, **7** xhibited moderate cytotoxicity, with cell viabilities of 80.9% at 10 μg·mL^{-1} and 77.6% at 20 μg·mL^{-1} (Table S5).

2.3. Anti-inflammatory effects *7*, *10*, and *11* on various models in vivo

We then evaluated the *in vivo* anti-inflammatory activities of **7**, **10**, and **11**. Ear piece weights of individual mice were measured before and after compound treatment to evaluate cutaneous inflammation. At a dose of 10 mg·kg^{-1}, **7**, **10**, and **11** inhibited croton oil-induced ear swelling in mice, with inhibition ratios of 49.7%, 57.3%, and 39.9% (Table S6), respectively.

Given that **10** showed the highest inflammatory activity, we further investigated its effects on pro-inflammatory factors in a mouse septicemia model. Compared with the negative control group, the levels of IL-6 and TNF-α showed a sharp increase in the model group. Treatment with **10** (10 mg·kg^{-1}) significantly inhibited the production of IL-6 and TNF-α from day 6 post-administration, and the effect was comparable to that of dexamethasone (2 mg·kg^{-1}) (Fig. S1).

Finally, we tested the effects of **10** on an adjuvant-induced arthritis (AIA) rat model. Visible erythema and swelling were observed in the hindpaws of AIA model rats. At 10 mg·kg^{-1}, **10** decreased the arthritis index and significantly alleviated swelling symptoms in knee joint circumference and hindpaws from day 6 after intraperitoneal administration (Fig. 5).

3. Conclusions

In summary, we isolated and structurally elucidated five new and four known sulfur-containing benzyl derivatives from the aqueous extracts of *G. elata*. **1** and **4** feature unusual sulfur-bearing polybenzyl moieties, while **3** is a unique sulfinate. We also synthesized four analogs, including two sulfones (**10** and **11**) and two disulfides (**12** and **13**). In *in vitro* anti-inflammatory bioassays, **7**, **10** and **11** dramatically inhibited LPS-induced production of IL-6 and TNF-α. On the *in vivo* inflammatory models, the synthesized sulfone **10** showed significant anti-inflammatory effects.

4. Experimental

4.1. General experimental procedures

Optical rotations were measured using a P-2000 polarimeter

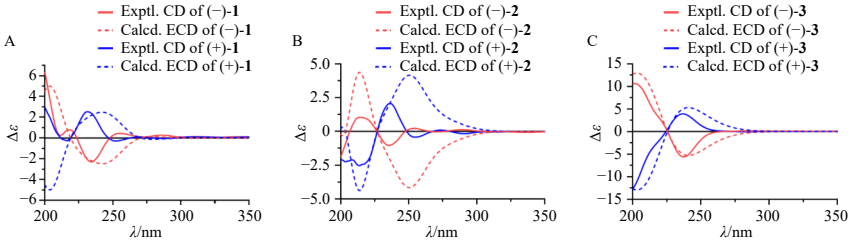

Fig. 4 Experimental and calculated ECD spectra for (±)-**1** (A), (±)-**2** (B), and (±)-**3** (C).

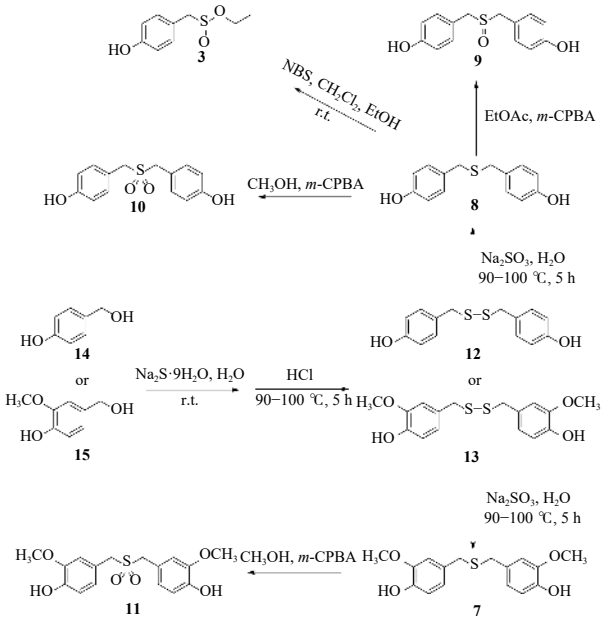

Scheme 1 Synthesis of **3** and **7**–**13**.

(JASCO, Tokyo, Japan). UV spectra were recorded on a V-650 spectrometer (JASCO, Tokyo, Japan). The CD spectra were measured on a JASCO J-815 spectropolarimeter (JASCO, Tokyo, Japan). IR spectra were recorded on a Nicolet 5700 FT-IR microscope transmission spectrometer (Thermo Electron Corporation, Madison, WI, USA). 1D and 2D NMR spectra were acquired at 600 or 500 MHz for ^{1}H and 150 or 125 MHz for ^{13}C, respectively, on SYS 600 MHz (Varian Associates Inc., Palo Alto, USA) or Bruker 500 (Bruker, Karlsruhe, Germany) spectrometers, with solvent peaks serving as references. ESI-MS and HR-ESI-MS data were measured using an Agilent 1100 Series LC-MSD-Trap-SL and an Agilent 6520 Accurate-Mass Q-TOFL CMS spectrometer (Agilent Technologies, Ltd., Santa Clara, CA, USA), respectively. Column chromatography (CC) was performed using macroporous adsorbent resin (HPD-110, Cangzhou Bon Absorber Technology Co., Ltd., Cangzhou, China), silica gel (200–300 mesh, Qingdao Marine Chemical Inc., Qingdao, China), Sephadex LH-20 (Pharmacia Biotech AB, Uppsala, Sweden), and MCI gel (CHP20P, 75–150 μm) (Mitsubishi Chemical Corporation, Tokyo, Japan). High-performance liquid chromatography (HPLC) separation was performed on an Agilent 1100 instrument (Agilent Technologies, Ltd., Santa Clara, CA, USA), using a Grace semi-preparative column packed with C_{18} reversed phase silica gel (250 mm × 10 mm, i.d. 5 μm) (Grace Inc., Columbia, SC, USA), or a Chiralpak AD-H column (250 mm × 10 mm, i.d. 5 μm) (Daicel Chiral Technologies Co., Ltd., Shanghai, China). Thin layer chromatography (TLC) was performed on glass precoated silica gel GF_{254} plates (Qingdao Marine Chemical Inc., Qingdao, China). Spots were visualized under UV light or by spraying with 5% H_2SO_4 in EtOH followed by heating. Unless otherwise noted, all chemicals were purchased from commercially available sources.

4.2. Plant material

For all details, please refer to reference [11].

4.3. Extraction and isolation

For the extraction and fractionation, please refer to references [3, 4, 6–8, 15]. The combined fractions C4 and C5 (6.8 g in total) were chromatographed on a silica gel column using an increasing gradient of acetone (0–100%) in petroleum ether to afford subfractions C4 + 5-1–C4 + 5-18. Subfraction C4 + 5-14 (94.5 mg) was crystalized from a mixture of petroleum ether–acetone (1∶1, *V*/*V*) to afford **9** (15.4 mg). Separation C4 + 5-6 (29 mg) was further separated on a Sephadex LH-20 column eluted with petroleum ether–CH_2Cl_2–MeOH (5∶5∶1, *V*/*V*/*V*), yielding C4 + 5-6-1 and C4 + 5-6-2. C4 + 5-6-1 was purified by RP-HPLC (C_{18} column, 50% MeOH in H_2O) to yield **3** (3.2 mg, t_R 15.4 min), which was further separated into (−)-**3** (1.6 mg, t_R 85.0 min) and (+)-**3** (1.6 mg, t_R 91.6 min) by semi-preparative HPLC (Chiralpak AD-H column, *n*-hexane–*i*PrOH, 9∶1, *V*/*V*). C4 + 5-7 (150 mg) was also separated on a Sephadex LH-20 column, eluted with petroleum ether–CH_2Cl_2–MeOH (5∶5∶1, *V*/*V*/*V*) to give C4 + 5-7-1–C4 + 5-7-3. C4 + 5-7-1 (8 mg) was further separated by the prepared TLC (CH_2Cl_2–MeOH, 30∶1, *V*/*V*) into C4 + 5-7-1-1 and C4 + 5-7-1-2. C4 + 5-7-1-2 (2.9 mg) was purified by RP-HPLC (C_{18} column, 60% MeOH in H_2O) to afford **6** (0.8 mg, t_R 14.5 min) and **7** (1.0 mg, t_R 10.4 min). C4 + 5-7-2 (6.7 mg) was separated by the prepared TLC (CH_2Cl_2–MeOH, 30∶1, *V*/*V*) into C4 + 5-7-2-1 and C4 + 5-7-2-2. C4 + 5-7-2-2 (1.5 mg) was purified by PR-HPLC (Grace C_{18} column, 60% MeOH in H_2O) to give **2** (1.6 mg, t_R 16.7 min). Chiral separation of **2** by a Chiralpak AD-H column (*n*-hexane–*i*PrOH, 3∶1, *V*/*V*) led to (−)-**2** (0.6 mg, t_R 63.5 min) and (+)-**2** (0.6 mg, t_R 68.7 min). C4 + 5-11 (371 mg) was separated over Sephadex LH-

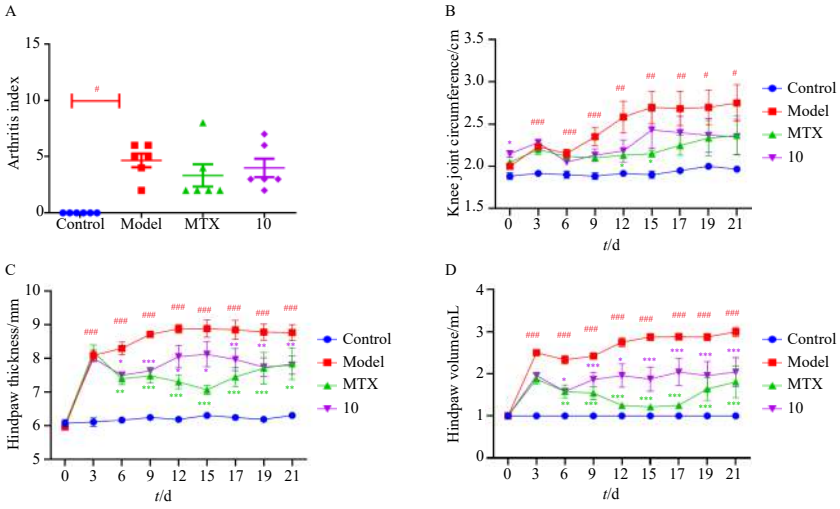

Fig. 5 Anti-inflammatory effects of **10** on the adjuvant induced rat arthritis model (mean ± SEM, *n* = 6). (A) Arthritis index; (B) Knee joint circumference (cm); (C) Hindpaw thickness (mm); (D) Hindpaw volume (mL). MTX: the positive drug methotrexate. $^{*}P < 0.05$, $^{**}P < 0.01$, $^{***}P < 0.001$ *vs* model group; $^{\#}P < 0.05$, $^{\#\#}P < 0.01$, $^{\#\#\#}P < 0.001$ *vs* control group.

20, eluted with petroleum ether–CH_2Cl_2–MeOH (5∶5∶1, *V/V/V*) to give C4 + 5-11-1–C4 + 5-11-5. C4 + 5-11-3 (10.2 mg) was purified by RP-HPLC (C_{18} column, 70% MeOH in H_2O) to yield **5** (1.4 mg, t_R 42.4 min). C4 + 5-11-5 (33.4 mg) was separated by the prepared TLC (CH_2Cl_2–MeOH, 15∶1, *V/V*) to yield C4 + 5-11-5-1–C4 + 5-11-5-5. C4 + 5-11-5-1 (16.2 mg) was further purified by RP-HPLC (C_{18} column, 70% MeOH in H_2O) to yield **1** (13 mg), which was further separated on a Chiralpak AD-H column, using *n*-hexane–*i*PrOH (3∶1, *V/V*) as the mobile phase to yield (+)-**1** (6.2 mg, t_R 26.5 min) and (−)-**1** (6.2 mg, t_R 29.7 min). C4 + 5-11-5-2 (1.3 mg) was purified by RP-HPLC (C_{18} column, 70% MeOH in H_2O) to afford **4** (1.1 mg, t_R 24.9 min). C4 + 5-11-5-5 (4.5 mg) was purified by RP-HPLC (C_{18} column, 60% MeOH in H_2O) to afford **8** (2.1 mg, t_R 30.7 min).

Gastrabenzylsulfoxide A (**1**): yellowish gum; $[\alpha]_D^{20}$ ≈ 0.0 (*c* 0.46, MeOH); UV (MeOH) λ_{max} (log ε) 204 (3.29), 232 (2.86), 280 (2.18) nm; IR ν_{max} 3289, 2925, 2697, 1686, 1612, 1513, 1444, 1368, 1210, 1150, 1109, 993, 896, 834, 803, 779, 725 cm^{-1}; ^1H NMR (acetone-d_6, 600 MHz) and ^{13}C NMR (acetone-d_6, 150 MHz) data (Table 1); ESI-MS: *m/z* 391 $[M + Na]^+$, 407 $[M + K]^+$, 367 $[M - H]^-$, 403 $[M + Cl]^-$; (+)-HR-ESI-MS: *m/z* 391.0991 $[M + Na]^+$ (Calcd. for $C_{21}H_{20}O_4SNa$, 391.0975). (+)-**1**: $[\alpha]_D^{20}$ +3.3 (*c* 0.86, MeOH); CD (MeOH) 232 ($\Delta\varepsilon_{232}$ +2.5); (−)-**1**: $[\alpha]_D^{20}$ −3.6 (*c* 0.93, MeOH); CD (MeOH) 235 ($\Delta\varepsilon_{235}$ −2.3).

Gastrabenzylsulfoxide B (**2**): white amorphous powder; $[\alpha]_D^{20}$ ≈ 0.0 (*c* 0.87, MeOH); UV (MeOH) λ_{max} (log ε) 203 (2.73), 235 (2.28), 281 (1.75) nm; IR ν_{max} 3366, 2920, 2850, 1712, 1666 (sh), 1611, 1515, 1453, 1374, 1274, 1174, 1157, 1127, 1030, 837, 799, 772, 740, 700 cm^{-1}; ^1H NMR (acetone-d_6, 600 MHz) and ^{13}C NMR (acetone-d_6, 150 MHz) data (Table 1); ESI-MS: *m/z* 315 $[M + Na]^+$; HR-ESI-MS: *m/z* 315.0667 $[M + Na]^+$ (Calcd. for $C_{15}H_{16}O_4SNa$, 315.0662). (+)-**2**: $[\alpha]_D^{20}$ +2.4 (*c* 0.05, MeOH); CD (MeOH) 236 ($\Delta\varepsilon_{236}$ +2.1); (−)-**2**: $[\alpha]_D^{20}$ −2.7 (*c* 0.05, MeOH); CD (MeOH) 236 ($\Delta\varepsilon_{236}$ −1.0).

Gastrabenzylsulfinate A (**3**): yellowish gum; $[\alpha]_D^{20}$ ≈ 0.0 (*c* 0.79, MeOH); UV (MeOH) λ_{max} (log ε) 203 (3.03), 232 (2.76), 279 (1.93) nm; IR ν_{max} 3321, 2984, 2926, 1680, 1614, 1597, 1517, 1449, 1387, 1233, 1203, 1137, 1107, 1013, 899, 872, 840, 802, 775, 722 cm^{-1}; ^1H NMR (acetone-d_6, 600 MHz) and ^{13}C NMR (acetone-d_6, 150 MHz) data (Table 1); ESI-MS: *m/z* 223 $[M + Na]^+$, 423 $[2M + Na]^+$; HR-ESI-MS: *m/z* 201.0577 $[M + H]^+$ (Calcd. for $C_9H_{13}O_3S$, 201.0580). (−)-**3**: $[\alpha]_D^{20}$ −18.1 (*c* 0.21, MeOH); CD (MeOH) 238 ($\Delta\varepsilon_{238}$ −5.6); (+)-**3**: $[\alpha]_D^{20}$ +16.3 (*c* 0.19, MeOH); CD (MeOH) 237 ($\Delta\varepsilon_{237}$ +3.9).

Gastrabenzylsulfide A (**4**): white amorphous powder; UV (MeOH) λ_{max} (log ε) 204 (3.57), 224 (sh, 3.16), 281 (1.43) nm; IR ν_{max} 3460, 2912, 1662 (sh), 1610, 1511, 1436, 1365, 1255, 1204, 1173, 1098, 1015, 951, 908, 891, 827, 776, 733 cm^{-1}; ^1H NMR (acetone-d_6, 600 MHz) and ^{13}C NMR (acetone-d_6, 150 MHz) data (Table 1); ESI-MS: *m/z* 481 $[M + Na]^+$, 497 $[M + K]^+$, 457 $[M - H]^-$, 493 $[M + Cl]^-$; HR-ESI-MS: *m/z* 481.1437 $[M + Na]^+$ (Calcd. for $C_{28}H_{26}O_4SNa$, 481.1444).

Gastrabenzylsulfide B (**5**): white amorphous powder; UV (MeOH) λ_{max} (log ε) 203 (2.86), 227 (2.63), 278 (1.83) nm; IR ν_{max} 3339, 2921, 1685 (sh), 1597, 1513, 1423, 1233, 1168, 1107, 1058, 1034, 836 cm^{-1}; ^1H NMR (acetone-d_6, 600 MHz) and ^{13}C NMR (acetone-d_6, 150 MHz) data (Table 1); ESI-MS: *m/z* 351 $[M - H]^-$; HR-ESI-MS: *m/z* 353.1214 $[M + H]^+$ (Calcd. for $C_{21}H_{21}O_3S$, 353.1206).

*4.4. Synthesis of **3** and **7**–**13***

*4.4.1. Synthesis of bis-(4-hydroxybenzyl)disulfide (**12**) and bis-(3-methoxy-4-hydroxybenzyl)disulfide (**13**)*

To a solution of $Na_2S{\cdot}9H_2O$ (80 mmol) in H_2O (200 mL), 6 N HCl (25 mL) and 4-hydroxybenzyl alcohol (**14**) or 4-hydroxy-3-methoxybenzyl alcohol (**15**) (40 mmol) were slowly added. The mixture was stirred for 5 h at 100 °C. After cooling to room temperature, the resulting solution was extracted with EtOAc (200 mL × 2), dried by anhydrous H_2SO_4, and purified by silica gel chromatography (PE–EtOAc, 2∶1) to yield bis-(4-hydroxybenzy1) disulfide (**12**, 70%) or bis-vanillyl disulfide (**13**, 75%). **12**: light yellow powder; ^1H NMR (acetone-d_6, 500 MHz) δ_H 8.33 (2H, s, O*H*-4/4'), 7.14 (4H, d, *J* = 8.5 Hz), 6.80 (4H, d, *J* = 8.5 Hz), 3.66 (4H, s); ^{13}C NMR (acetone-d_6, 125 MHz) δ_C 157.6, 131.3, 128.9, 115.9, 43.0; (−)-HR-ESI-MS *m/z* 277.0361 $[M - H]^-$ (Calcd. for $C_{14}H_{13}O_2S_2$, 277.0351). **13**: light yellow powder; ^1H NMR (acetone-d_6, 500 MHz) δ_H 7.57 (2H, s, *OH*-4/4'), 6.89 (2H, d, *J* = 2.0 Hz), 6.77 (2H, dd, *J* = 8.5, 2.0 Hz), 6.76 (2H, dd, *J* = 8.5 Hz), 3.85 (6H, s, 3/3'-OC*H*$_3$), 3.67 (4H, s); ^{13}C NMR (acetone-d_6, 125 MHz) δ_C 148.2, 147.0, 129.6, 123.1, 115.7, 113.8, 56.3 (-O*C*H$_3$), 43.7; (−)-HR-ESI-MS *m/z* 337.0577 $[M - H]^-$ (Calcd. for $C_{16}H_{17}O_4S_2$, 337.0563).

*4.4.2. Synthesis of bis-vanillyl sulfide (**7**) and bis-(4-hydroxybenzyl) sulfide (**8**)*

Compound **13** (2.96 mmol) or **12** (3.60 mmol) was dissolved in H_2O (40 mL), followed by the addition of Na_2SO_3 (7.14 mmol). The reaction mixture was stirred for 5 h at 100 °C, slowly cooled to room temperature, and further stirred for 1 h at 0–5 °C. After filtration, the filter cake was washed with water (5 mL × 2), and dried by air at 40 °C to obtain **8** (71%) or **7** (84%). **7**: white powder; ^1H NMR (acetone-d_6, 500 MHz) δ_H 7.46 (2H, s, O*H*-4/4'), 6.89 (2H, br s), 6.76 (4H, br s), 3.59 (4H, s); ^{13}C NMR (acetone-d_6, 125 MHz) δ_C 148.1, 146.4, 130.7, 122.4, 115.5, 113.2, 56.2 (-O*C*H$_3$), 36.2; (+)-HR-ESI-MS: *m/z* 329.0809 $[M + Na]^+$ (Calcd. for $C_{16}H_{18}O_4SNa$, 329.0810) [23]. **8**: white powder; ^1H NMR (acetone-d_6, 500 MHz) δ_H 8.27 (2H, s, O*H*-4/4'), 7.17 (4H, d, *J* = 8.5 Hz), 6.82 (4H, d, *J* = 8.5 Hz), 3.60 (4H, s); ^{13}C NMR (acetone-d_6, 125 MHz) δ_C 156.1, 129.8, 128.3, 115.1, 34.6; (−)-HR-ESI-MS *m/z* 245.0635 $[M - H]^-$ (Calcd. for $C_{14}H_{13}O_2S$, 245.0642) [24].

*4.4.3. Synthesis of bis-(4-hydroxybenzyl)sulfone (**10**) and bis-(3-methoxy-4-hydroxybenzyl)sulfone (**11**)*

Compound **8** (0.92 mmol) or **7** (0.92 mmol) was dissolved in methanol (10 mL), followed by the slow addition of *m*-CPBA (2.02 mmol). The reaction mixture was stirred at room temperature for 3 h. Methanol was then removed under reduced pressure at 40 °C. The residue was re-dissolved in CH_2Cl_2 (10 mL), stirred at room temperature for 1 h and then cooled to 0–5 °C for 1 h. The mixture was filtered, washed with dichloromethane (2 mL × 2), and dried to obtain **10** (82%) or **11** (75%). **10**: light yellow powder; ^1H NMR (acetone-d_6, 500 MHz) δ_H 8.49 (2H, s, O*H*-4/4′), 7.25 (4H, d, *J* = 9.0 Hz), 6.85 (4H, d, *J* = 9.0 Hz), 4.19 (4H, s); ^{13}C NMR (acetone-d_6, 125 MHz) δ_C 158.1, 132.8, 118.6, 115.8, 57.1; (−)-HR-ESI-MS *m/z* 277.0537 $[M - H]^-$ (Calcd. for $C_{14}H_{13}O_4S$, 277.0529). **11**: light yellow powder; ^1H NMR (acetone-d_6, 500 MHz) δ_H 7.74 (2H, s, O*H*-4/4′), 7.01 (2H, dd, *J* = 3.5, 7.5 Hz), 6.88 (2H, d, *J* = 7.5 Hz), 6.85 (2H, d, *J* = 3.5 Hz), 4.22 (2H, s), 4.21 (2H, s), 3.84 (6H, s, 3/3'-OC*H*$_3$); ^{13}C NMR (acetone-d_6, 125 MHz) δ_C 148.3, 147.9, 125.0, 120.5, 115.8, 115.3, 58.1, 56.3 (-O*C*H$_3$); (−)-HR-ESI-MS *m/z* 337.0752 $[M - H]^-$ (Calcd. for $C_{16}H_{17}O_6S$, 337.0740).

*4.4.4. Synthesis of **3***

Compound **8** (1.00 mmol) was dissolved in CH_2Cl_2 (20 mL), followed by the addition of NBS (1.20 mmol) and ethanol (1.0 mL). The mixture was stirred at room temperature for 2 h. **3** (51%) was obtained *via* silica gel column chromatography (PE–EtOAc, 1∶1).

*4.4.5. Synthesis of **9***

Compound **8** (0.92 mmol) was dissolved in CH_2Cl_2 (10 mL),

and *m*-CPBA (0.92 mmol) was slowly added. The reaction mixture was stirred at room temperature for 1 h and then cooled to 0–5 °C for 1 h. After filtration, the filter cake was washed with CH_2Cl_2 (2 mL × 2), and dried at 40 °C to obtain **9** (78%). **9**: white solid; ^{1}H NMR (acetone-d_6, 500 MHz) δ_H 9.58 (2H, s, O*H*-4/4'), 7.15 (4H, d, *J* = 8.0 Hz), 6.77 (4H, d, *J* = 8.0 Hz), 4.25 (4H, s); ^{13}C NMR (acetone-d_6, 125 MHz) δ_C 157.6, 132.3, 118.1, 115.3, 56.6 [11]; (+)-HR-ESI-MS: *m/z* 263.0736 $[M + H]^+$ (Calcd. for $C_{14}H_{15}O_3S$, 263.0736).

4.5. ECD calculations

ECD calculations for (±)-**1**, (±)-**2**, and (±)-**3** were performed as previously described [7].

4.6. Anti-inflammatory activities assays

4.6.1. In vitro activity against IL-6 and TNF-α

BV-2 cells were cultured in Dulbecco's modified Eagle's medium (DMEM) supplemented with 10% fetal bovine serum (FBS), 100 U·mL^{-1} penicillin, 100 μg·mL^{-1} streptomycin, and 5.5 mmol·L^{-1} glucose at 37 °C under 5% CO_2 and 95% humidity. To evaluate the influence of test compounds on the production of IL-6 and TNF-α, BV-2 cells were preincubated with varying concentrations of tested compounds (10, 1, 0.1 μg·mL^{-1}) for 1 h, followed by stimulation with LPS (1 μg·mL^{-1}) for 24 h. Post-incubation, the culture supernatants from the BV-2 cells were harvested and subsequently analyzed using commercial enzyme-linked immunosorbent assay (ELISA) kits according to the manufacturer's instructions (Thermo Fisher Scientific, Waltham, MA, USA). The optical density (OD) at 450 nm was measured using an ELISA plate reader (Synergy H1, BioTek, USA).

4.6.2. Cell viability assay

BV2 cells were seeded in a 96-well plate (5 × 10^4/mL) for adherence. The cells were then treated with various concentrations of the test compounds for 24 h. Subsequently, CCK8 solution was added to each well (10 μL/well) and incubated for an additional 2 h. Absorbance was measured at 450 nm using a microplate reader. The relative cell viability was calculated as a percentage of the control group.

4.6.3. Croton-oil-induced ear edema mouse model

The protocol used was as previously reported [25]. Briefly, ICR mice were adaptively raised for one week before being randomly divided into different groups: the model group and treatment groups administered 10 compounds at a dose of 10.0 mg·kg^{-1} (*n* = 10). Intraperitoneal injection dosages were calculated based on body weight at 0.1 mL/10 g, with the model group receiving an equivalent volume of solvent on the day of the experiment. Prior to administration, the animals underwent a fasting period of 5 to 6 h. One hour after intraperitoneal injection, a 2% (*V*/*V*) croton oil mixture was evenly applied to the front and back of the mouse's right ear, using 50 μL to induce inflammation. The left ear served as a self-control without any inflammatory agent applied to calculate the swelling rate. After 4 h of modeling with the croton oil mixture, the animals were sacrificed, both ears were removed, and an ear piece was punched at the same position on each ear. The weight of each ear piece was recorded to calculate the ear swelling rate using the formula: Ear swelling rate (%) = [(right ear piece weight − left ear piece weight)/left ear piece weight] × 100. Inhibition rate of ear swelling (%) = [(swelling rate of model group − swelling rate of administration group)/swelling rate of control group] × 100.

4.6.4. LPS injection-induced septicemia

The model was executed as previously described [26]. C57BL/6 mice were randomly assigned to five groups (*n* = 5), including a control or sham group, an LPS-treated model group, a group treated with 5 or 10 mg·kg^{-1} of **10**, and a dexamethasone treated group (2 mg·kg^{-1}). To induce the LPS-induced septicemia model, mice were intraperitoneally injected with LPS (10 mg·kg^{-1}). Survival was monitored for 72 h until no further deaths occurred. Blood samples were collected at 4, 6, and 24 h post-LPS injection and stored at −80 °C for further analysis.

4.6.5. Rat adjuvant-induced arthritis (AIA) model

SD rats were randomly divided into four groups (*n* = 6): a control group, a model group, a positive drug methotrexate group (1 mg·kg^{-1}), and a group treated with **10** (10 mg·kg^{-1}). Rats in the model and treatment groups received intradermal injections of 100 μL of Freund's complete adjuvant on the left hind foot plantar surface. Intraperitoneal administration commenced on the first day after modeling. Measurements of the left knee joint circumference, hindpaw thickness, and hindpaw volume were taken every three days. Starting from the 13th day post-modeling, rats exhibited gradual development of secondary reactions. The disease score of clinical symptoms were evaluated by two independent observers.

Funding

This work was supported by the National Natural Science Foundation of China (No. 82293680), the National Science and CAMS Innovation Fund for Medical Science (No. 2021-I2M-1-028), and the Nonprofit Central Research Institute Fund of Chinese Academy of Medical Sciences (No. 2021-RC350-009).

Supporting information

Method for ECD calculation of the stereoisomers of **1**–**3**, bioassay protocols, 1D and 2D NMR spectra, HR-ESI-MS, IR, UV, and ECD data for new compounds **1**–**5**, 1D NMR spectra for the synthetic compounds **2**, **3**, and **7**–**13**, are available in the Supporting information, and can be requested by sending E-mail to the corresponding author.

Declaration of competing interest

These authors have no conflict of interest to declare.

References

1 Gong MQ, Lai FF, Chen JZ, et al. Traditional uses, phytochemistry, pharmacology, applications, and quality control of *Gastrodia elata* Blume: a comprehensive review. *J Ethnopharmacol*. 2024;319:117128. https://doi.org/10.1016/j.jep.2023.117128.
2 Su Z, Yang Y, Chen S, et al. The processing methods, phytochemistry and pharmacology of *Gastrodia elata* Bl.: a comprehensive review. *J Ethnopharmacol*. 2023;314:116467. https://doi.org/10.1016/j.jep.2023.116467.
3 Xu CB, Guo QL, Wang YN, et al. Gastrodin derivatives from *Gastrodia elata*. *Nat Prod Bioprospect*. 2019;9(6):393-404. https://doi.org/10.1007/s13659-019-00224-1.
4 Wang YN, Zhang M, Zhou X, et al. Insight into medicinal chemistry behind traditional Chinese medicines: *p*-hydroxybenzyl alcohol-derived dimers and trimers from *Gastrodia elata*. *Nat Prod Bioprospect*. 2021;11(1):31-50. https://doi.org/10.1007/s13659-020-00258-w.
5 Chen SY, Geng CA, Ma YB, et al. Polybenzyls from *Gastrodia elata*, their agonistic effects on melatonin receptors and structure-activity relationships. *Bioorg Med Chem*. 2019;27(15):3299-3306. https://doi.org/10.1016/j.bmc.2019.06.008.
6 Guo QL, Wang YN, Lin S, et al. 4-Hydroxybenzyl-substituted amino acid derivatives from *Gastrodia elata*. *Acta Pharm Sin B*. 2015;5(4):350-357. https://doi.org/10.1016/j.apsb.2015.02.002.
7 Guo QL, Wang YN, Zhu CG, et al. 4-Hydroxybenzyl-substituted glutathione derivatives from *Gastrodia elata*. *J Asian Nat Prod Res*. 2015;17(5):439-454. https://doi.org/10.1080/10286020.2015.1040000.
8 Guo QL, Lin S, Wang YN, et al. Gastrolatathioneine, an unusual ergothioneine derivative from an aqueous extract of "Tian Ma": a natural product co-produced by plant and symbiotic fungus. *Chin Chem Lett*. 2016;27(10):1577-1581. https://doi.org/10.1016/j.cclet.2016.06.040.
9 Huang NK, Chern Y, Fang JM, et al. Neuroprotective principles from *Gastrodia*

elata. *J Nat Prod*. 2007;70(4):571-574. https://doi.org/10.1021/np0605182.
10 Pyo MK, Jin JL, Koo YK, et al. Phenolic and furan type compounds isolated from *Gastrodia elata* and their anti-platelet effects. *Arch Pharm Res*. 2004;27(4):381-385. https://doi.org/10.1007/BF02980077.
11 Hye SYC, Pyo MK. Isolation of 4,4′-dihydroxybenzyl sulfoxide from *Gastrodia elata*. *Arch Pharm Res*. 1997;20:91-92. https://doi.org/10.1007/BF02974050.
12 Liu CM, Tian ZK, Zhang YJ, et al. Effects of gastrodin against lead-induced brain injury in mice associated with the Wnt/Nrf2 pathway. *Nutrients*. 2020;12(6):1805. https://doi.org/10.3390/nu12061805.
13 Zhang XL, Yuan YH, Shao QH, et al. DJ-1 regulating PI3K-Nrf2 signaling plays a significant role in bibenzyl compound 20C-mediated neuroprotection against rotenone-induced oxidative insult. *Toxicol Lett*. 2017;271:74-83. https://doi.org/10.1016/j.toxlet.2017.02.022.
14 Wang S, Han QW, Zhou TT, et al. A bibenzyl compound 20C protects rats against 6-OHDA-induced damage by regulating adaptive immunity associated molecules. *Int Immunopharmacol*. 2021;91:107269. https://doi.org/10.1016/j.intimp.2020.107269.
15 Huang JY, Yuan YH, Yan JQ, et al. 20C, a bibenzyl compound isolated from *Gastrodia elata*, protects PC12 cells against rotenone-induced apoptosis *via* activation of the Nrf2/ARE/HO-1 signaling pathway. *Acta Pharmacol Sin*. 2016;37(6):731-740. https://doi.org/10.1038/aps.2015.154.
16 Mou Z, Yuan YH, Lou YX, et al. Bibenzyl compound 20C protects against endoplasmic reticulum stress in tunicamycin-treated PC12 cells *in vitro*. *Acta Pharmacol Sin*. 2016;37(12):1525-1533. https://doi.org/10.1038/aps.2016.75.
17 Shao S, Xu CB, Chen CJ, et al. Divanillyl sulfone suppresses NLRP3 inflammasome activation *via* inducing mitophagy to ameliorate chronic neuropathic pain in mice. *J Neuroinflamm*. 2021;18(1):142. https://doi.org/10.1186/s12974-021-02178-z.
18 Ye TY, Meng XB, Zhai YD, et al. Gastrodin ameliorates cognitive dysfunction in diabetes rat model *via* the suppression of endoplasmic reticulum stress and NLRP3 inflammasome activation. *Front Pharmacol*. 2018;9:1346. https://doi.org/10.3389/fphar.2018.01346.
19 Li XF, Xiang B, Shen T, et al. Anti-neuroinflammatory effect of 3,4-dihydroxybenzaldehyde in ischemic stroke. *Int Immunopharmacol*. 2020;82:106353. https://doi.org/10.1016/j.intimp.2020.106353.
20 Cao X, Cao L, Zhang WC, et al. Therapeutic potential of sulfur-containing natural products in inflammatory diseases. *Pharmacol Therapeut*. 2020;216:107687. https://doi.org/10.1016/j.pharmthera.2020.107687.
21 Wang N, Saidhareddy P, Jiang XF. Construction of sulfur-containing moieties in the total synthesis of natural products. *Nat Prod Rep*. 2020;37(2):246-275. https://doi.org/10.1039/c8np00093j.
22 Nagasawa S, Fujiki S, Sasano Y, et al. Chromium–Salen complex/nitroxyl radical cooperative catalysis: a combination for aerobic intramolecular dearomative coupling of phenols. *J Org Chem*. 2021;86(9):6952-6968. https://doi.org/10.1021/acs.joc.1c00438.
23 Pons A, Floch M, Shinkaruk S, et al. Identification and organoleptic contribution of vanillylthiol in wines. *J Agric Food Chem*. 2016;64(6):1318-1325. https://doi.org/10.1021/acs.jafc.5b05733.
24 Xiao YQ, Li L, You XL. Studies on chemical constituents of effective part of *Gastrodia elata*. *Chin J Chin Mater Med*. 2002;27(1):35-36.
25 Zang YD, Lai FF, Fu JM, et al. Novel nitric oxide-releasing derivatives of triptolide as antitumor and anti-inflammatory agents: design, synthesis, biological evaluation, and nitric oxide release studies. *Eur J Med Chem*. 2020;190:112079. https://doi.org/10.1016/j.ejmech.2020.112079.
26 Fu JM, Zang YD, Zhou Y, et al. A novel triptolide derivative ZT01 exerts anti-inflammatory effects by targeting TAK1 to prevent macrophage polarization into pro-inflammatory phenotype. *Biomed Pharmacother*. 2020;126:110084. https://doi.org/10.1016/j.biopha.2020.110084.